Fluctuation-induced tricritical points

Daniel Blankschtein*
Department of Electronics, The Weizmann Institute of Science, Rehovot 76100, Israel and Department of Physics and Astronomy, Tel Aviv University, Tel Aviv 69978, Israel

Amnon Aharony
Department of Physics and Astronomy, Tel Aviv University, Tel Aviv 69978, Israel
(Received 17 September 1982)

In the vicinity of a tricritical point an n-component spin system is shown to have continuous transitions which are driven by fluctuations (they would be first order according to Landau's theory). We show that spin anisotropies which imply crossover to lower symmetry (e.g., of m-component spins with $m<n$) may turn these fluctuation-driven continuous transitions first order via tricritical points. In cubic systems, which exhibit fluctuation-driven first-order transitions, the anisotropy may yield two consecutive tricritical points. We present a detailed renormalization-group analysis of these situations with emphasis on the importance of the sixth-order terms in the Ginzburg-Landau-Wilson continuous-spin Hamiltonian. A list of possible experimental realizations is also given.

I. INTRODUCTION

In most cases Landau's theory[1] provides a correct qualitative description of phase transitions. The main effect of fluctuations emphasized in the last few decades is to change critical exponents and details near critical and multicritical points. Modern critical phenomena theory has given a general explanation for these new features, associating them with fixed points of the renormalization-group (RG) transformations.[2,3] A second effect of fluctuations which has been less emphasized is to move phase boundaries in the parameter space. For example, the critical line of a simple second-order transition is shifted to lower temperatures (compared to Landau-theory prediction).[2] Although this shift is not universal, i.e., it depends on all the parameters in the Hamiltonian (including the "irrelevant" ones), it has important practical implications.

Similarly, one expects shifts in the borderlines between regions of continuous and discontinuous transitions, i.e., in tricritical borderlines.[4–8] We have recently[9] emphasized such shifts for isotropic n-component spin tricritical lines, and discussed the "fluctuation-driven *continuous* transitions," i.e., transitions which are predicted by Landau's theory to be first order but are turned by fluctuations to become continuous. The "opposite" effect, of "fluctuation-driven *first-order* transitions" has been earlier found to occur whenever a stable fixed point of the RG does not exist or is out of reach.[3,10–14]

A very useful tool in the study of critical phenomena has been the application of symmetry-breaking fields.[3] In particular, breaking the symmetry between different spin components (by a "quadratic anisotropy") yields the well-studied bicritical phase diagram observable, e.g., in anisotropic antiferromagnets under a magnetic field,[15] in structural transitions under uniaxial stress,[16] etc. Several recent theoretical papers[17–20] observed that a quadratic anisotropy may turn fluctuation-driven first-order transitions back into continuous ones. This effect was indeed observed in MnO (Ref. 21) and in $RbCaF_3$.[22] In a recent paper[9] we discussed the "inverse" effect, in which fluctuation-driven continuous transitions are turned first order by anisotropy. We also mentioned briefly the possibility that there may exist a region in the parameter space for which the anisotropy first turns the fluctuation-driven first-order transition into a continuous one, and then turns it back into first order via two consecutive tricritical points. The aim of the present paper is to give the full details of these calculations.

Our analysis is based on a RG study of the continuous Ginzburg-Landau-Wilson n-component spin model.[2,3] Sec. II contains a detailed discussion of fluctuation-driven continuous transitions. We emphasize the importance of the sixth-order terms in the Ginzburg-Landau-Wilson expansion, and show that such transitions will always occur near *tricritical* points of *isotropic* n-component spin systems. In Sec. III we show that when this happens, application of a quadratic symmetry-breaking field g turns the transition *first order* again at a *tricritical* point, which is subsequently located using a large quadratic anisotropy expansion. In Sec. IV we analyze the small quadratic anisotropy limit and use RG methods to calculate universal amplitude ratios characterizing the tricritical points. In systems which exhibit fluctuation-driven first-order transitions, increasing g may yield two consecutive tricritical points. A well-studied example of fluctuation-driven first-order transitions concerns systems with *cubic symmetry*.[3,14] In Sec. V we discuss such systems with much detail and show that it is possible to map the n-component cubic model, with sixth-order terms included, into one of cubic symmetry in which these are absent. This procedure enables us to locate the tricritical points with the use of the well-known critical behavior of the truncated cubic model. In Sec. IV we apply the large quadratic anisotropy limit to locate the new tricritical points. Section VII is devoted to a preliminary RG analysis in which we present qualitative arguments to show the existence of two consecutive tricritical points. The analysis contains a new discussion of the effects of the sixth-order cubic terms near the cubic fixed point. In Sec. VIII we discuss possible experimental realizations of the new effects predicted in this paper. Section IX contains our conclusions.

II. FLUCTUATION-DRIVEN CONTINUOUS PHASE TRANSITIONS

To understand the origins of fluctuation-driven continuous transition consider the usual isotropic Ginzburg-Landau-Wilson (GLW) Hamiltonian for n-component spins $[\vec{S}(\vec{x})]$ in d dimensions,[2,3]

$$\mathscr{H}=\int d^dx[\tfrac{1}{2}\,|\vec{\nabla}\vec{S}\,|^2+\tfrac{1}{2}r\,|\vec{S}\,|^2+u_4\,|\vec{S}\,|^4+u_6\,|\vec{S}\,|^6+O(\,|\vec{S}\,|^8)]\;, \tag{1}$$

where $r\sim T-T_L$ (T_L being the Landau transition temperature) and u_4, u_6, etc., are assumed to be almost temperature independent. The model (1) with $u_4 \lesssim 0$ and $u_6>0$ (for thermodynamic stability) may be used to describe *tricritical*[4] behavior. Landau showed[1] that in the absence of fluctuations (1) yields (i) a *first-order* transition for $u_4<0$ and $u_6>0$ at $r=u_4^2/2u_6$, (ii) a *continuous* transition for $u_4>0$ at $r=0$ (in this case u_6 is unimportant), and (iii) a *tricritical point* for $u_4=0$ ($u_6>0$) at $r=0$.

To incorporate the effects of fluctuations and study the quantitative changes they induce in the phase diagram we use the RG approach.[2,3] Although we are concerned mainly with the *tricritical* behavior of (1), we construct differential RG recursion relations[5] which will enable us to go beyond the tricritical region, associated with the Gaussian fixed point (for $d\geq 3$, see below), and study the *critical* region associated with the Heisenberg fixed point (for $d \lesssim 4$, see below), as well. With this in mind, and keeping terms of appropriate order, the flow of r, u_4, and u_6 (assumed to be small) under the differential RG transformation is found to be[6]

$$\frac{dr}{dl}=2r+4(n+2)K_d u_4(1-r)\;, \tag{2}$$

$$\frac{du_4}{dl}=(4-d)u_4+3(n+4)K_d u_6 -4(n+8)K_d u_4^2\;, \tag{3}$$

$$\frac{du_6}{dl}=(6-2d)u_6-12(n+14)K_d u_6 u_4\;, \tag{4}$$

where

$$K_d^{-1}=2^{d-1}\pi^{d/2}\Gamma(d/2)\;.$$

Note that in Eqs. (2)—(4) we have deliberately left the d dependence in various terms and in K_d. This is done to emphasize that the results to be obtained concerning tricriticality (associated with the Gaussian fixed point) will be correct not only for $d \lesssim 4$ but rather for $3\leq d<4$ (see below). In Eq. (2) we have expanded the propagator factor as $(1+r)^{-1}\simeq 1-r$, and in Eqs. (3) and (4) we have replaced $(1+r)^{-2}$ by unity because as long as $r \lesssim O(1)$ the solutions are not affected to $O(u_4,u_6)$. Note that to leading order u_6 does *not* generate new contributions to r [Eq. (2)] under the differential RG iterations (these would involve *two independent* momentum integrations over infinitesimal shells of width δl and therefore vanish in the limit $\delta l\to 0$). On the other hand, from Eq. (3) it is clear that under the RG iterations u_6 *does generate* new contributions to u_4, which implies that the correct quartic scaling field $\tilde{u}_4$ is a combination of u_4 and u_6 given by

$$\tilde{u}_4=u_4+C(n)u_6\;,\qquad C(n)=3(n+4)K_d/(d-2)\;. \tag{5}$$

To leading order in u_6, Eqs. (3) and (5) yield

$$\frac{d\tilde{u}_4}{dl}=(4-d)\tilde{u}_4-4(n+8)K_d\tilde{u}_4^2\;. \tag{6}$$

To this order one may also replace u_4 by $\tilde{u}_4$ in Eq. (4). Replacing u_4 by $[\tilde{u}_4-C(n)u_6]$ in Eq. (2), we find that the temperature scaling field

$$t=r+2(n+2)K_d[u_4+3(n+4)K_d u_6/2(d-2)]$$

obeys the equation

$$\frac{dt}{dl}=2t-4(n+2)K_d\tilde{u}_4 t\;. \tag{7}$$

The set of Eqs. (4), (6), and (7) possesses a trivial Gaussian fixed point ($t^G=\tilde{u}_4^G=u_6^G=0$) at any d. In particular, for $3<d<4$, this fixed point has *two* *relevant* scaling fields t and u_4 (with eigenvalues $\lambda_t^G=2$ and $\lambda_4^G=4-d$, respectively) and an *irrelevant one* u_6 (with $\lambda_6^G=6-2d$). Note that at $d=3$, u_6 becomes marginal, yielding logarithmic corrections.[7] Thus, the *doubly unstable* Gaussian fixed point is expected to describe tricriticality for $3\le d<4$. The equations also yield a (nontrivial) Heisenberg fixed point of order $\epsilon=4-d$, i.e., $t^H=0$, $u_6^H=0$, and $\tilde{u}_4^H=\epsilon/4(n+8)K_d$. In particular, for $d\lesssim 4$, this point has *one relevant* scaling field $\tilde{t}$ (with $\lambda_t^H=2-[(n+2)/(n+8)]\epsilon$) and *two irrelevant* ones, $\Delta\tilde{u}_4=\tilde{u}_4-\tilde{u}_4^H$ and u_6 (with $\lambda_4^H=-\epsilon$ and $\lambda_6^H=-2-[(n+26)/(n+8)]\epsilon$, respectively). The *singly unstable* isotropic Heisenberg fixed point is therefore expected to describe criticality for $d\lesssim 4$.

If we were interested only in the tricritical region, then it would be sufficient to concentrate in the close vicinity of the Gaussian fixed point, i.e., $\tilde{u}_4\simeq 0$, $u_6\simeq 0$, and $t\simeq 0$. In that limit, and for $3<d<4$, Eqs. (4), (6), and (7) with only the linear terms become *exact*, yielding Gaussian exponents. However, to approach criticality, it is necessary to include the nonlinear terms. The solutions of Eqs. (4), (6), and (7) applicable in both the tricritical and critical regions (taking the appropriate limits, see below) are given to $O(u_4,u_6)$ by[6]

$$t(l)=t(0)e^{2l}/Q(l)^{(n+2)/(n+8)}\,,$$

$$t(0)=r+2(n+2)K_d\times[u_4+3(n+4)K_d u_6/2(d-2)]\,, \quad (8)$$

$$\tilde{u}_4(l)=\tilde{u}_4(0)e^{(4-d)l}/Q(l)\,, \qquad \tilde{u}_4(0)=u_4+C(n)u_6 \quad (9)$$

$$u_6(l)=u_6 e^{(6-2d)l}/Q(l)^{3(n+14)/(n+8)}\,, \qquad u_6>0 \quad (10)$$

where

$$Q(l)=1+[\tilde{u}_4(0)/\tilde{u}_4^H](e^{\epsilon l}-1)\,. \quad (11)$$

Note that the factor $Q(l)$ in (11) reflects the Gaussian-to-Heisenberg crossover. In the limit $\tilde{u}_4(0)=\tilde{u}_4^H$, one has $Q(l)=e^{\epsilon l}$, yielding the Heisenberg-type critical behavior. On the other hand, in the limit $\tilde{u}_4(0)\ll\tilde{u}_4^H$, one has $Q(l)\simeq 1$, yielding the Gaussian-type tricritical behavior.

Equations (8) and (9) show that for $\tilde{u}_4(0)>0$ and $t(0)=0$ the Hamiltonian flow evolves towards the Heisenberg fixed point, yielding a *continuous* phase transition. On the other hand, for $\tilde{u}_4(0)<0$ the stable fixed point is *not accessible.* Iteration up to $t(l)\simeq 1$ and matching to the Landau theory then yields a *first-order* transition.[6,14] The point $t(0)=0,\tilde{u}_4(0)=0$ is therefore *tricritical,* marking the borderline between these two regimes. In terms of the original variables (u_4,u_6) this implies that fluctuations shift the line of tricritical points $u_4=0$, $u_6>0$ (predicted by Landau theory) down to $\tilde{u}_4(0)=0$,[6–9] see Fig. 1.

Comparison with the Landau result ($u_4=0$) now shows that in the range $-C(n)u_6<u_4<0$ we can consider the continuous phase transitions as being driven by critical fluctuations. The crucial role played by u_6 has been ignored in many earlier RG calculations. Although technically *irrelevant* (in the RG sense) for $d\gtrsim 3$ [see Eq. (10)], $u_6>0$ is essential for stability whenever $u_4<0$, and must therefore be included in the RG analysis. We would like to emphasize that the irrelevance of u_6 manifests itself primarily in its incapability to affect the asymptotic critical behavior of the system.

III. ISOTROPIC MODEL IN THE LIMIT OF LARGE QUADRATIC ANISOTROPY

We now add the *quadratic anisotropy,*

$$\mathscr{H}_g=\tfrac{1}{2}g\int d^dx[m\,|\vec{S}_{n-m}|^2-(n-m)\,|\vec{S}_m|^2]/n\,, \quad (12)$$

where $\vec{S}_{n-m}$ and $\vec{S}_m$ are the $(n-m)$- and m-component parts of the vector $\vec{S}$ which will generate a crossover from the n-component critical behavior to that of the m- [or $(n-m)$-] component one for $g>0$ (<0).[3] This follows simply from the fact that for $g=0$, there is a *single* temperaturelike variable r for all the n components, whereas for $g\neq 0$ there are *two*: (i) $r_m=r-[(n-m)/n]g$ for the first m components, and (ii) $r_{n-m}=r+[m/n]g$ for the remaining $(n-m)$. Therefore, for $g>0$ $(g<0)$ the m-$[(n-m)$-] component correlation length ξ_m (ξ_{n-m}) diverges at criticality, while ξ_{n-m} (ξ_m) remains finite. For convenience we consider only $g>0$, the results for $g<0$ being obtainable by replacing $g\rightarrow -g$ and $m\rightarrow n-m$.

If $u_4>0$ then Eq. (12) generates the *bicritical*

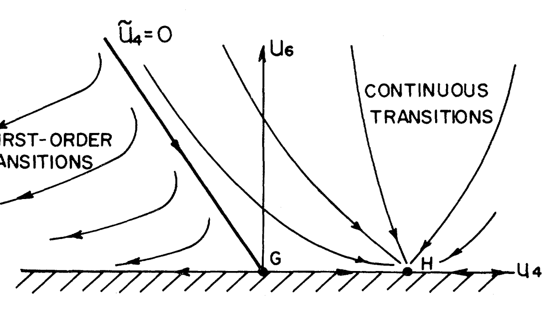

FIG. 1. Schematic RG flow diagram in the (u_4,u_6) critical plane for $d\lesssim 4$. Line of tricritical points $\tilde{u}_4(0)=0$ is associated with the Gaussian fixed point (G). Points to the right of this line flow to the stable Heisenberg fixed point (H). Cross-hatched region $(u_6<0)$ is unphysical.

phase diagram[3] shown in Fig. 2(a). Bicritical phase diagrams are predicted both by Landau and RG theories; the only effects of fluctuations are (i) to shift T_L down to T_B (bicritical temperature), and (ii) to induce a *tangential* (instead of a finite slope) approach of the continuous transition lines to the T axis at the bicritical point $T=T_B, g=0$.

In this section we show that in the range $-C(n)u_6<u_4<-C(m)u_6$, the application of the anisotropy field g (>0) may turn the fluctuation-driven continuous transition expected for the n-component system back into first order beyond some tricritical points [Figs. 2(b) and 2(c)].

For $g \gg 1$, the fluctuations in the $(n-m)$ components of $\vec{S}_{n-m}$ become small, i.e., $r_{n-m} \gg r_m$, and we can integrate $\vec{S}_{n-m}$ our of the partition function using a perturbation expansion in powers of u_4 and u_6 to obtain the effective m-component spin Hamiltonian[17]

$$\mathscr{H}_{\text{eff}} = \int d^d x [\tfrac{1}{2} |\vec{\nabla} \vec{S}_m|^2 + \tfrac{1}{2} r_{\text{eff}} |\vec{S}_m|^2 + u_4^{\text{eff}} |\vec{S}_m|^4 + u_6^{\text{eff}} |\vec{S}_m|^6 + O(|\vec{S}_m|^8)] , \quad (13)$$

where to leading order in u_4 and u_6 one has

$$r_{\text{eff}} = r_m + O(u_4, u_6) = r - [(n-m)/n]g + O(u_4, u_6) , \quad (14)$$

$$u_4^{\text{eff}} = u_4 + 3(n-m) I_1(r_{n-m}) u_6 - 4(n-m) I_2(r_{n-m}) u_4^2 + O(u_4 u_6, u_6^2) , \quad (15)$$

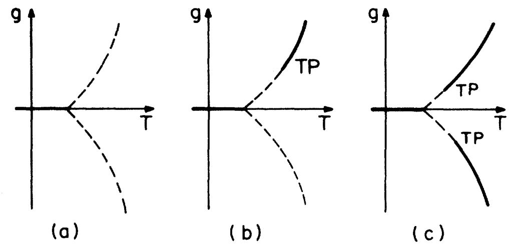

FIG. 2. Schematic (g,T) phase diagrams. Dashed (solid) lines represent continuous (first-order) transitions. TP is a tricritical point. Transitions for $g>0$ ($g<0$) are into an m- [$(n-m)$-] component phase (we chose $m<n-m$). (a), (b), and (c) correspond, respectively, to $u_4>-C(m)u_6$, $-C(m)u_6>u_4>-C(n-m)u_6$, and $-C(n-m)u_6>u_4>-C(n)u_6$.

$$u_6^{\text{eff}} = u_6 + O(u_4 u_6, u_6^2, u_4^3) , \quad (16)$$

with

$$r_{n-m} = r + [m/n] g$$

and

$$I_k(x) = \int \frac{d^d q}{(2\pi)^d} \frac{1}{(x+q^2)^k} .$$

The effective m-component Hamiltonian (13) will have a tricritical point at $\tilde{u}_4^{\text{eff}}=0$ [see Eq. (5)], i.e.,

$$\tilde{u}_{4,t}^{\text{eff}} = [u_4^{\text{eff}} + C(m) u_6^{\text{eff}}]_t = \tilde{u}_{4,t} + 3(n-m)[I_1(r_{n-m}) - K_d/(d-2)] u_6 - 4(n-m) I_2(r_{n-m}) u_4^2 = 0 . \quad (17)$$

The integrals $I_1(x)$ and $I_2(x)$ are *monotonically decreasing* with x. However, for $x \gg 1$ (i.e., for sufficiently large g) one has $I_2(x) \ll I_1(x)$. If in addition $-C(n)u_6<u_4<-C(m)u_6$, then $\tilde{u}_4^{\text{eff}}$ will change sign as function of g, becoming negative for sufficiently large g (see Fig. 3). For very large x, one has

$$I_k(x) = [K_d/d] x^{-k} - [k K_d/(d+2)] x^{-k-1} + O(x^{-k-2}) .$$

Keeping terms of $O(x^{-2})$, Eq. (17) may, in principle, have *two* solutions (corresponding to *two* possible tricritical points); however, in the large-g limit only *one* of these is acceptable. In Sec. IV we shall see that in systems with cubic symmetry the existence of an additional quartic variable may yield *two* acceptable solutions, i.e., two consecutive tricritical points. In the present case, the tricritical point occurs at

$$g_t \simeq -3(n-m) K_d u_6 / d[u_4 + C(m) u_6] . \quad (18)$$

Note that the validity of (18) in the large-g limit implies that $u_4+C(m)u_6 \lesssim 0$; therefore, strictly speaking, we have only demonstrated the existence of (18) for $u_4 \lesssim -C(m)u_6$.

Up to this point we assumed that u_4 (and u_6) does not depend explicitly on g. In general, such a dependence could lead to a change in the sign of u_4. If this happens, then Figs. 2(b) and 2(c) could arise trivially even in the context of Landau's theory. However, in that case the phase diagrams would not exhibit the amplitude ratios listed below. In most practical cases, the direct dependence of u_4 on g is weak. In the next section we shall complement (18) by finding the shape of the tricritical curve for small g [Eq. (29)].

IV. RG ANALYSIS OF THE TRICRITICAL REGION

In this section we shall demonstrate the occurrence of tricritical points at small anisotropy fields ($g \ll 1$) in the region $0 < u_4 + C(n)u_6 \ll \tilde{u}_4^H$ [i.e., in the limit when $Q(l) \simeq 1$; see (11)]. As explained in Sec. III the integration over $\vec{S}_{n-m}$ is justified only when $r_{n-m} \gg r_m$ [or equivalently $r_{n-m} \simeq O(1)$ while $r_m \simeq 0$]. For small g in the critical region $r_m \simeq r - O(g) \simeq 0$ we also have $r_{n-m} = r + O(g) \ll 1$, showing that fluctuations in all n components are almost equally important. A naive attempt to eliminate $\vec{S}_{n-m}$ in this case will produce infrared divergences at small momenta[6,23] resulting from the fluctuations in $\vec{S}_{n-m}$. A rather direct way to overcome this difficulty is to use the RG recursion relations to map the almost critical initial Hamiltonian $\mathscr{H}$ into a Hamiltonian $\mathscr{H}(l)$. The basic idea behind this approach is to choose $l = l^*(t,g)$ such that $\mathscr{H}(l^*)$ is noncritical with respect to fluctuations in $\vec{S}_{n-m}$, i.e., $r_{n-m}(l^*) \simeq O(1)$. At l^*, a simple perturbation theory in powers of $u_4(l^*)$ and $u_6(l^*)$ (see Sec. III) can be used to eliminate $\vec{S}_{n-m}$ (for a review on this approach see Ref. 23), obtaining an effective m-component Hamiltonian of exactly the same form as (13) in which all the coefficients are l^* dependent. At this stage the tricritical point is found as in Sec. III. The solutions of the RG recursion relations are subsequently used to express the answers (obtained in terms of the Hamiltonian parameters at l^*) as functions of the original parameters (at $l=0$).

When $g \gtrsim 0$, the GLW Hamiltonian for n-component spins $[\vec{S}(\vec{x})]$ in d dimensions is given by

$$\mathscr{H} = \int d^d x \Big[\tfrac{1}{2} |\vec{\nabla}\vec{S}|^2 + \tfrac{1}{2} r_m |\vec{S}_m|^2 + \tfrac{1}{2} r_{n-m} |\vec{S}_{n-m}|^2 + u_4 |\vec{S}|^4 + u_6 |\vec{S}|^6 + O(|\vec{S}|^8) \Big] , \quad (19)$$

where r_m and r_{n-m} were defined before. Under iterations of the RG to leading order in u_4 and u_6 the renormalized Hamiltonians $\mathscr{H}(l)$ remain in the parameter space (r_m, r_{n-m}, u_4, u_6). To $O(u_4, u_6)$ the differential recursion relations for $r_m(l)$ are[23]

$$\frac{dr_m}{dl} = 2r_m + 4(m+2)K_d u_4(1-r_m) + 4(n-m)K_d u_4(1-r_{n-m}) , \quad (20)$$

$$\frac{dr_{n-m}}{dl} = 2r_{n-m} + 4(n-m+2)K_d u_4(1-r_{n-m}) + 4mK_d u_4(1-r_m) . \quad (21)$$

Provided that $r_m(l)$ and $r_{n-m}(l)$ do not become too large [i.e., $r_i(l) \lesssim O(1)$], one may assume that the isotropy of the fourth- and sixth-order terms $u_4(l)$ and $u_6(l)$ in (19) is conserved. This means that the RG flows in the (u_4, u_6) plane are not affected to $O(u_4, u_6)$ by the breaking of the isotropic quadratic symmetry, which implies that Eqs. (3) and (4) for $u_4(l)$ and $u_6(l)$, respectively, are still applicable. In order to solve Eqs. (20) and (21) we reintroduce the original variables r and g [see Eqs. (1) and (12)]. The evolution of r is then dictated again by Eq. (2), and that of g is dictated by

$$\frac{dg}{dl} = 2g - 8K_d \tilde{u}_4 g , \quad (22)$$

where to leading order in u_6 we have replaced u_4 by $\tilde{u}_4$ [see Eq. (5)]. The solution of (22) is[23]

$$g(l) = g e^{2l} / Q(l)^{2/(n+8)} , \quad (23)$$

with $Q(l)$ given in (11). Note that in the limit $\tilde{u}_4(0) \ll \tilde{u}_4^H$, i.e., $Q(l) \simeq 1$, one recovers the Gaussian exponent $\lambda_g^G = 2$.

Having solved the recursion relations, we select a value of l^* by requiring[6,23]

$$r_{n-m}(l^*) = 1 + O(u_4, u_6) . \quad (24)$$

At this point the renormalized Hamiltonian $\mathscr{H}(l^*)$ is noncritical with respect to fluctuations in $\vec{S}_{n-m}$. Thus the trace over $\vec{S}_{n-m}$ can be performed precisely as in Sec. III, yielding the effective Hamiltonian (13). The various parameters in (13), which now depend on l^*, are given by Eqs. (14)–(16). In $\mathscr{H}_{\text{eff}}(l^*)$ we easily identify a temperaturelike variable [see Eq. (8)],

$$t_{\text{eff}} = r_{\text{eff}} + 2(m+2)K_d \times [u_4^{\text{eff}} + 3(m+4)K_d u_6^{\text{eff}} / 2(d-2)] .$$

Tricriticality (t) will be obtained when $t_{\text{eff},t} = \tilde{u}_{4,t}^{\text{eff}} = 0$. To leading order, the condition $t_{\text{eff},t} = 0$ yields

$$t_{\text{eff},t} = r_{m,t}(l^*) + O(u_4, u_6) \simeq t_t(l^*) - [(n-m)/n] g_t(l^*) = 0 , \quad (25)$$

with $t(l)$ and $g(l)$ given by (8) and (23), respectively. To satisfy (24) at tricriticality it is sufficient to impose

$$t_t(l^*) + [m/n] g_t(l^*) = 1 , \quad (26)$$

which, with the use of the definition of $r_{n-m}(l^*)$, ensures the validity of (24). The condition $\tilde{u}_{4,t}^{\text{eff}} = 0$ is given [see Eq. (17)] by

$$\tilde{u}_{4,t}^{\text{eff}} = [u_4^{\text{eff}}(l^*) + C(m) u_6^{\text{eff}}(l^*)]_t = \tilde{u}_{4,t}(l^*) + 3(n-m)[I_1(r_{n-m}(l^*)) - K_d/(d-2)] u_6(l^*) = 0 , \quad (27)$$

where we have neglected the term of $O(u_4^2)$ in (17). Note that to leading order in u_6, $r_{n-m}(l^*)$ in I_1 can be replaced by unity [see Eq. (24)].

If the n-component Hamiltonian (1) is almost tricritical, then one has $\tilde{u}_4(0)\simeq 0$ or equivalently $\tilde{u}_4(0)/\tilde{u}_4^H \ll 1$, which implies $Q(l^*)\simeq 1$. In that case, as mentioned before, one recovers the Gaussian model and Eqs. (8)—(10) and (23) reduce, respectively, to $t(l)=t(0)\exp[2l]$ with

$$t(0)=[T-T_B(g=0)]/T_B(g=0)$$

given in (8),

$$\tilde{u}_4(l)=\tilde{u}_4(0)\exp[(4-d)l] ,$$

$$u_6(l)=u_6\exp[(6-2d)l] ,$$

and $g(l)=g\exp[2l]$. Subtracting (25) from (26) we obtain $g(l^*)\simeq 1$, which implies

$$e^{l^*}\simeq g^{-1/2} . \tag{28}$$

Inserting the values for $\tilde{u}_4(l^*)$, $u_6(l^*)$, and $\exp(l^*)$ into (27), we obtain

$$\tilde{u}_{4,t}=[u_4+C(n)u_6]_t=B_m g_t^{\psi} , \tag{29}$$

with

$$\psi=\tfrac{1}{2}d-1$$

and (30)

$$B_m=[3K_d/(d-2)-3I_1(1)](n-m)u_6 .$$

A similar expression with B_{n-m} and $-g_t$ replacing B_m and g_t is obtained for $g<0$. We have therefore shown that as function of g, the tricritical point ($\tilde{u}_4=0$ at $g=0$) splits into two tricritical lines (Fig. 3) which emerge from it tangentially ($\psi<1$ in $3\leq d<4$ dimensions) to the u_4 axis. The universal ratio B_m/B_{n-m} is given by

$$B_m/B_{n-m}=(n-m)/m . \tag{31}$$

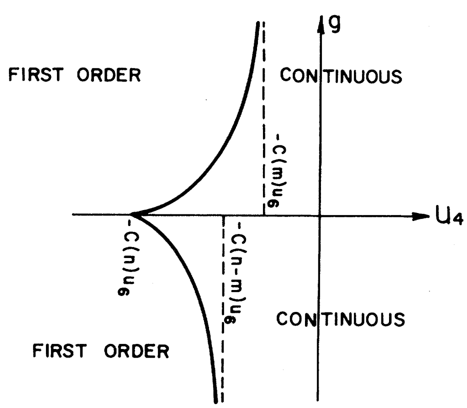

FIG. 3. Schematic (g,u_4) phase diagram with $m<n-m$. Heavy (tricritical) lines separate regions of continuous and first-order transitions.

Using Eq. (25) and the definitions for $t(l^*)$, $g(l^*)$, and $\exp(l^*)$ given above, we can locate the tricritical points in Figs. 2(b) and 2(c). For $g>0$ [Fig. 2(b)] the tricritical point is given by

$$g_t=A_m t_t^{\phi} , \tag{32}$$

where

$$t_t=[T_t(g)-T_t(g=0)]/T_t(g=0) ,$$

$$\phi=\lambda_g^G/\lambda_t^G=1 , \tag{33}$$

and

$$A_m=n/(n-m) .$$

A similar expression with A_{n-m} and $-g_t$ replacing A_m and g_t is obtained for $g<0$. The universal ratio A_m/A_{n-m} is given by

$$A_m/A_{n-m}=m/(n-m) . \tag{34}$$

These results are valid for $3<d<4$. At $d=3$ they may be modified by logarithmic corrections,[7] and the exponents ψ and ϕ describing the curves in the (u_4,g) and (g,t) planes, respectively, will have a different dependence on d for $d<3$.[8]

One can summarize our discussion in terms of the Hamiltonian flows. We start above the line $\tilde{u}_4=u_4+C(n)u_6=0$ in the (u_4,u_6) plane (Fig. 1), i.e., when the n-component system exhibits continuous phase transitions, and iterate l^* times. For sufficiently large g almost no iterations are needed to reach $r_{n-m}\simeq 1$ and to eliminate $\vec{S}_{n-m}$. Therefore $l^*\simeq 0$ and a trajectory's length (which is related to l^*) is very *short*. In that case the flow ends *below* the m-component tricritical line, i.e., $u_4+C(m)u_6<0$, and the m-component transition becomes *first order*. On the other hand, for small g a *large* value of l^* is needed and the flow *crosses the* m-component tricritical line, ending *above* this line. In that case the m-component transition remains continuous. Hence, we expect that for some value g_t the flow will reach precisely the m-component tricritical line, yielding a tricritical point.

V. TRICRITICALITY IN SYSTEMS WITH CUBIC ANISOTROPY

The best-studied example of fluctuation-driven first-order transitions is that of systems with cubic symmetry.[3,24] We therefore limit our discussions to this example. We start by replacing Eq. (1) by

$$\mathcal{H}=\mathcal{H}_I+\mathcal{H}_C , \tag{35}$$

where $\mathscr{H}_I$ is the usual isotropic GLW Hamiltonian given in Eq. (1) and $\mathscr{H}_C$ is given by

$$\mathscr{H}_C=\int d^dx \left[v\sum_{\alpha=1}^{n} S_\alpha^4 + x\sum_{\alpha=1}^{n} S_\alpha^6 + y\sum_{\alpha=1}^{n}\sum_{\substack{\beta=1\\ \beta\neq\alpha}}^{n} S_\alpha^4 S_\beta^2 + O(|\vec{S}|^8)\right] . \quad (36)$$

The parameters v, x, and y are assumed to be almost temperature independent.

In the present paper we concentrate on the case $v<0$ and in Sec. IX discuss only briefly the case $v>0$. The critical properties of the cubic model with positive definite quartic terms were reviewed, e.g., in Refs. 3 and 25. As long as the quartic terms are positive definite, i.e., $u_4+v>0$ ($v<0$), Landau's theory[1] predicts a continuous phase transition at $r=0$ (in that case the sixth-order terms are unimportant). Moreover, the symmetry of the ordered phase is determined only by the sign of v.[25] The tetragonal (TE) phase (ordering along a cube axis) occurs for $v<0$, while a trigonal (TR) one (ordering along a cube diagonal) occurs for $v>0$. First-order transitions are predicted when the quartic terms are *negative,* i.e., $u_4+v<0$ ($v<0$). In that case higher-order terms are essential for the stability of the free energy and may play a role in the determination of the possible ordered phases. In the simplest case, an additional orthorhombic (OR) phase (ordering along a cube face diagonal) is possible due to the competition between the fourth- and sixth-order terms. For example, the $n=3$ cubic crystal $BaTiO_3$ (Ref. 26) undergoes a sequence of three first-order transitions, the first one being into a TE phase (the additional phases are OR and TR). Our assumptions that $u_4+v>0$, $v<0$, ensure (within Landau's theory) a continuous transition into the TE phase.

For a TE distortion Landau's theory predicts tricriticality at $r=0$, $u_4+v=0$ ($v<0$), and $u_6+x>0$ (for stability). As shown in Ref. 3, in the absence of sixth-order terms, fluctuations tend to shift the tricritical boundary into $u_4+3v/(4-n)$ for $v<0$. This shift generates a region in the (u_4,$v<0$) plane in which, although the Landau stability criterion $u_4+v>0$ is fulfilled, the stable (for $n<4$) isotropic (Heisenberg) fixed point is inaccessible, resulting in fluctuation-driven first-order transitions.[14] If one starts below the classical (Landau) instability boundary ($u_4+v<0$) of the n-component system, or if (after symmetry breaking) the resulting effective m- [or $(n-m)$-] component Hamiltonian has negative fourth-order terms, it is crucial to include positive sixth-order terms for stability of the free energy.

In the preceding sections we have seen that the Gaussian fixed point describes correctly the tricritical behavior of an isotropic system not only for $d\leq 4$, but rather in the whole range $3\leq d<4$. In the cubic case, however, the tricritical behavior (for $v<0$) is associated with the cubic fixed point[3,24,14] which is of $O(\epsilon)$. Therefore, to incorporate the effects of fluctuations in the cubic case we apply RG methods in $d=4-\epsilon$ dimensions and assume that u_4 and v are of $O(\epsilon)$ (initially and throughout their flow).[17]

Consider the Hamiltonian (35) with u_4 and v of order $\epsilon=4-d$. To leading order in ϵ the renormalized Hamiltonians $\mathscr{H}(l)$ (under the RG iterations) remain in the original parameter space (r,u_4,v,u_6,x,y). To this order, and to $O(u_6,x,y)$, the RG differential recursion relations for $r(l)$, $u_4(l)$, $u_6(l)$, $x(l)$, and $y(l)$ are found to be

$$\frac{dr}{dl}=2r+4(n+2)K_4u_4(1-r)+12K_4v(1-r) , \quad (37)$$

$$\frac{du_4}{dl}=\epsilon u_4-4(n+8)K_4u_4^2-24K_4u_4v+3(n+4)K_4u_6+6K_4y , \quad (38)$$

$$\frac{dv}{dl}=\epsilon v-36K_4v^2-48K_4u_4v+15K_4x+(n-7)K_4y , \quad (39)$$

$$\frac{du_6}{dl}=(-2+2\epsilon)u_6-12(n+14)K_4u_6u_4-36K_4u_6v-24K_4yu_4 , \quad (40)$$

$$\frac{dx}{dl}=(-2+2\epsilon)x-180K_4xu_4-180K_4xv-144K_4u_6v-4(n-7)K_4yu_4 , \quad (41)$$

$$\frac{dy}{dl}=(-2+2\epsilon)y-4(n+23)K_4yu_4-84K_4yv-60K_4xu_4-144K_4u_6v , \quad (42)$$

with $K_4=1/8\pi^2$. Note that in the limit $(v,x,y)\to 0$, i.e., the *isotropic* case, Eqs. (2)–(4) are recovered. Also, u_6, x, and y *do not* generate new contributions to r (see Sec. III). On the other hand, from Eqs. (38) and (39) it is evident that under the RG iterations u_6, x, and y *do* generate new contributions to u_4 and v. Following the arguments of Sec. III it is possible to eliminate these contributions by defining two new quartic scaling fields, $\tilde{u}_4$ and $\tilde{v}$, given to $O(u_6,x,y)$ by

$$\tilde{u}_4 = u_4 + C(n)u_6 + C_2(n)y\ , \tag{43}$$

$$\tilde{v} = v + C_1(n)x + C_3(n)y\ , \tag{44}$$

with

$$C(n) = \frac{3}{2-\epsilon}(n+4)K_4,\quad C_1(n) = \frac{15}{2-\epsilon}K_4\ ,$$
$$C_2(n) = \frac{6}{2-\epsilon}K_4,\quad C_3(n) = \frac{1}{2-\epsilon}(n-7)K_4\ . \tag{45}$$

In terms of $\tilde{u}_4$ and $\tilde{v}$, Eqs. (39) and (40) are replaced to leading order in u_6, x, and y by

$$\frac{d\tilde{u}_4}{dl} = \epsilon\tilde{u}_4 - 4(n+8)K_4\tilde{u}_4^2 - 24K_4\tilde{u}_4\tilde{v}\ , \tag{46}$$

$$\frac{d\tilde{v}}{dl} = \epsilon\tilde{v} - 36K_4\tilde{v}^2 - 48K_4\tilde{u}_4\tilde{v}\ . \tag{47}$$

Note that Eqs. (46) and (47) are precisely those which describe the evolution of the quartic variables ($\tilde{u}_4$ and $\tilde{v}$) in the usual n-component cubic system without sixth-order terms.[3] This "mapping" from (u_4,v) to $(\tilde{u}_4,\tilde{v})$ via transformations (43) and (44) enables us to extract the critical properties of the cubic model with sixth-order terms from those of the same model without them. Note that a similar transformation, $u_4 \to \tilde{u}_4$ [Eq. (5)], was performed in the isotropic case.

For $\tilde{v}<0$, the tricritical boundary in the $(\tilde{u}_4,\tilde{v})$ plane is given by $W(n)=0$, with

$$W(n) = \tilde{u}_4 + 3\tilde{v}/(4-n) = u_4 + 3v/(4-n) + C(n)u_6 + B(n)x + A(n)y\ , \tag{48}$$

where

$$A(n) = C_2(n) + 3C_3(n)/(4-n)\ ,$$
$$B(n) = 3C_1(n)/(4-n)/(4-n)\ , \tag{49}$$

and $C(n)$ is given in (45). Equation (48) represents a surface in five-dimensional (u_4, $v<0$, u_6,x,y) critical (i.e., $T=T_B$) space. Points *below* this surface will exhibit first-order transitions (no accessible fixed point), points *on* it will show tricritical behavior associated with the cubic fixed point ($u_4^C, v_C, u_6^C = x_C = y_C = 0$), and points *above* it will undergo continuous transitions associated (for $n<4$) with the stable isotropic (Heisenberg) fixed point ($u_4^H, v_H = u_6^H = x_H = y_H = 0$). Since it is almost impossible to visualize a five-dimensional space we present a schematic diagram showing the location of the n- [and m-] component tricritical planes (for $v<0$) in the tridimensional subspace (u_4,v,u_6, $x=y=0$) as predicted by RG theory.

Figure 4 shows that the two tricritical planes $W(n)=0$ (plane n) and $W(m)=0$ (plane m) intersect at line α. This intersection generates two regions, a and b, in the (u_4,v,u_6) subspace. In the full five-dimensional parameter space the tricritical planes become four-dimensional hypersurfaces which intersect at a three-dimensional "line." In what follows we shall not need the explicit equation of this line.

VI. THE CUBIC MODEL IN THE LARGE-ANISOTROPY LIMIT

We now consider the cubic system with quadratic anisotropy, adding Eq. (12) to Eq. (35). In the absence of the sixth-order terms Ref. 17 predicted that if the n-component system has a fluctuation-driven first-order transition (close to its tricritical point) then the anisotropy may yield the phase diagram of Fig. 5(a). We shall now show that the sixth-order terms may turn Fig. 5(a) into Figs. 5(b) or 5(c).

As before, we start with the large-g limit. For $g \gg 1$ fluctuations in the $(n-m)$-components of $\vec{S}_{n-m}$ are small and can be integrated out of the partition function following the methods outlined in Sec. III. As a result we obtain the following effective m-component cubic Hamiltonian:

$$\mathcal{H}_{\text{eff}} = \mathcal{H}^I_{\text{eff}} + \mathcal{H}^C_{\text{eff}}\ , \tag{50}$$

where $\mathcal{H}^I_{\text{eff}}$ is the effective m-component isotropic Hamiltonian given in (13) and $\mathcal{H}^C_{\text{eff}}$ is an effective m-component cubic Hamiltonian given by

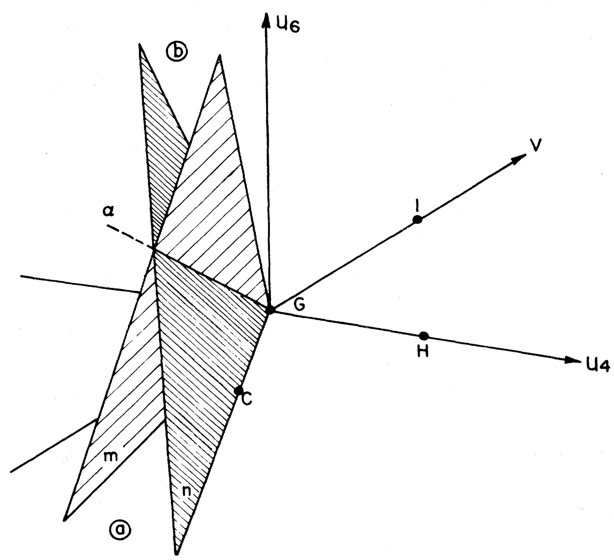

FIG. 4. Schematic RG diagram showing the location of the n- (m-) component tricritical plane denoted as n (m). Planes intersect at line α. Cubic (C), Heisenberg (H), Ising (I), and Gaussian (G) fixed points are shown. For visual clarity we did not include the RG flows.

$$\mathscr{H}^{C}_{\rm eff}=\int d^dx\left[v_{\rm eff}\sum_{\alpha=1}^{m}S_\alpha^4+x_{\rm eff}\sum_{\alpha=1}^{m}S_\alpha^6+y_{\rm eff}\sum_{\alpha=1}^{m}\sum_{\substack{\beta=1\\ \beta\neq\alpha}}^{m}S_\alpha^4S_\beta^2+O(|\vec{S}|^8)\right]. \tag{51}$$

To leading order in u_4, v, u_6, x, and y we find

$$v_{\rm eff}\simeq v+(n-m)yI_1(r_{n-m}), \tag{52}$$

$$x_{\rm eff}\simeq x,\ \ y_{\rm eff}\simeq y . \tag{53}$$

The equations for $u_4^{\rm eff}$ [(15)] and $u_6^{\rm eff}$ [(16)] remain unchanged, and that for $r_{\rm eff}$ is given by (14) with the additional contribution $12(n-m)K_4I_1^2(r_{n-m})y$. Note that Eq. (52) raises the possibility that $v_{\rm eff}$ may change sign as function of g if v and y have different signs (this would imply $y\gg -v$). Such a situation needs further investigation. We shall therefore assume in what follows that the sign of $v_{\rm eff}$ is controlled by that of v. In that case the Hamiltonian (50) will exhibit tricritical behavior [Eq. (48)] at $W_{\rm eff}(m)=0$, with

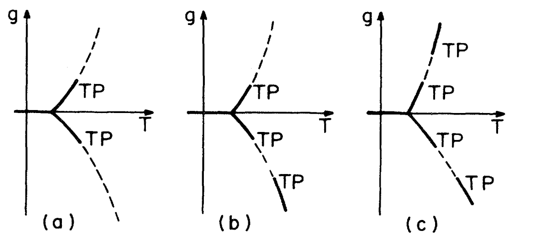

FIG. 5. Schematic (g,T) phase digrams for the cubic case, with $v<0$. The value of u_4 decreases from (a) to (c) and notation is as in Fig. 2.

$$W_{\rm eff}(m)=W(m)+3(n-m)I_1(r_{n-m})[u_6+y/(4-m)]-4(n-m)I_2(r_{n-m})u_4^2 , \tag{54}$$

with

$$W(m)=u_4+3v/(4-m)+C(m)u_6+B(m)x+A(m)y$$

[see Eqs. (48) and (49)]. If one starts just below the m-component tricritical plane (outside region a, see Fig. 4), i.e., $W(m)\lesssim 0$ and in addition $u_6+y/(4-m)>0$ (more complex situations could be realizable; however, these need further investigation), then $W_{\rm eff}(m)$ will change sign *twice* as a function of r_{n-m} (or equivalently of g). For sufficiently large g one has $W_{\rm eff}(m)\simeq W(m)\lesssim 0$ and the transition is first order. As g is lowered, there is a range in which $I_1(x)\gg I_2(x)$ (see Sec. III) and the second (*positive*) term in (54) may overcome both $W(m)$ and the last (*negative*) term, so that $W_{\rm eff}(m)\gtrsim 0$ and the transition becomes continuous beyond a tricritical point. Lowering g further (still in the range $g\gg 1$) the last (*negative*) term may finally dominate the behavior of $W_{\rm eff}(m)$, making it *negative* once more beyond a second tricritical point, i.e., the transition becomes first order again [see Figs. 5(b) and 5(c)]. It follows, then, that one may expect the occurrence of two consecutive tricritical points; however, one must still check that both of them are compatible with the assumption of very large g (note that a similar argument was presented in Sec. III for the isotropic case where we checked and found that only *one* tricritical point fulfilled the above mentioned requirement.)

Following Sec. III we expand $I_k(r_{n-m})$, $k=1,2$ [in Eq. (54)] in powers of r_{n-m}^{-1} to order r_{n-m}^{-2}. Denoting the tricritical value $r_{n-m,t}^{-1}\equiv R_t$, we find

$$a(u_4,u_6,y)R_t^2+b(u_6,y)R_t+W(m)\simeq 0 , \tag{55}$$

with

$$a(u_4,u_6,y)=-(n-m)K_4[2u_4^2+u_6+y/(4-m)]/2 ,$$
$$b(u_6,y)=3(n-m)K_4[u_6+y/(4-m)]/4 , \tag{56}$$

and $W(m)$ given in Eqs. (39) and (49). Note that in the present calculation we have assumed $g>0$, and therefore only *positive* ($R_t>0$) solutions of (55) are acceptable. Moreover, our previous assumption $u_6+y/(4-m)>0$ ensures that $b>0$ and $a<0$ [see (56)]. In the limit $g\gg 1$ (or equivalently $r_{n-m}\gg 1$) one has $0<R\ll 1$, which indicates that only those roots of (55) which are positive and small are compatible with our assumptions. Equation (55) will yield two positive solutions

$$R_{t1}=(-b/2a)[1+\Delta^{1/2}]$$

and

$$R_{t2}=(-b/2a)[1-\Delta^{1/2}] ,$$

with $\Delta=1-4(a/b)[W(m)/b]$ for $1\geq\Delta\geq 0$. For $\Delta=0$, i.e., $W(m)\equiv W^*=b^2/4a$, one has $R_{t1}=R_{t2}=-b/2a$. For $\Delta=1$, i.e., $W(m)=0$, one has $R_{t1}=-b/a$, $R_{t2}=0$. One positive solution $R_t=R_{t1}$ is obtained for $\Delta>1$, i.e., $W(m)>0$, and no real solution exists for $\Delta<0$, i.e., $W(m)<W^*$. We thus find two consistent solutions if $|b/a|\ll 1$ and

$b/a \geq 4W(m)/b$. The simplest way to fulfill both requirements is to choose x and y of $O(u_6)$, $u_4 \gg u_6$, and $u_4+3v/(4-m) \lesssim 0$ (i.e., $W(m) \to 0^-$). Note that in the isotropic case (Sec. III), the simultaneous existence of R_{t1} and R_{t2} would have implied $u_4 \gg u_6$ and $u_4 \simeq -C(m)u_6$ [i.e., $W(m) \to 0^-$], which are evidently incompatible. It is only the existence of the additional quartic variable v which enables the simultaneous fulfillment of both requirements, thus making it possible to obtain two tricritical points. In terms of g the two tricritical points are located at

$$g_{t1}=(-2a/b)[1+\Delta^{1/2}]^{-1}\,,$$
$$g_{t2}=(-2a/b)[1-\Delta^{1/2}]^{-1}\,. \tag{57}$$

To summarize the large-g limit calculation, we present in Fig. 6 lines of tricritical points in the (g,u_4) plane for increasing values of u_6 (with x and y set to zero for simplicity). When $u_6=0$ (solid lines), one has $b=0$ in Eq. (55). In that case the problem reduces to the usual cubic one treated in Ref. 17. There is a *single* tricritical point at $g_t=[-a/W(m)]^{1/2}$ which exists only for $W(m) \geq 0$, i.e., $u_4 \geq -3v/(4-m)$, and terminates at the $(g=0)$ n-component tricritical point (point A in Fig. 6). The limit $g \to 0^+$ will be discussed in Sec. VII where we show that the lines of tricritical points approach the u_4 axis tangentially. For $u_6=0$ $(u_6 \neq 0)$ this occurs at point A (B) of Fig. 6. By turning on

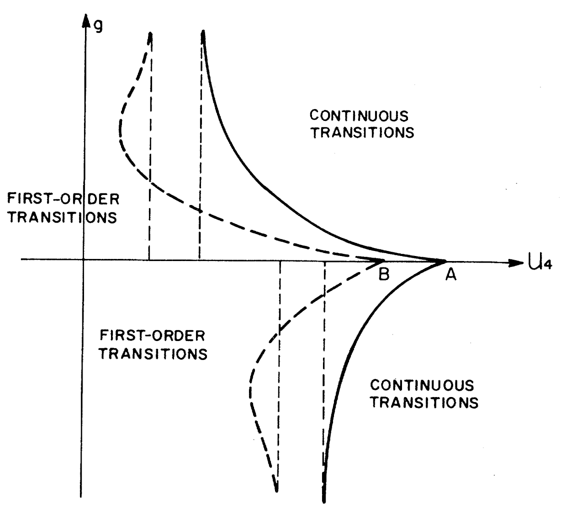

FIG. 6. Schematic (g,u_4) phase diagram with $m<n-m$ for $u_6>0$, $x=y=0$. Tricritical lines (solid lines for $u_6=x=y=0$ and dashed lines for $u_6>0$, $x=y=0$) separate regions of continuous (above the lines) and first order (below the lines) transitions. Limiting values of u_4, for $|g_t| \to \infty$, are given by $W(m)=0$. Points A and B correspond to $W(n)=0$.

$u_6>0$ the lines of tricritical points (dashed lines in Fig. 6) are shifted towards more negative values of u_4 (in particular, for $g=0$, point A is shifted to point B). As explained before, a *single* tricritical point g_t is obtained for $0>W(n)$, $W(m)>0$. In the range $W^* < W(m) \leq 0$ *two* tricritical points g_{t1} and g_{t2} are obtained. Note that the region of continuous transitions enclosed by the region of first-order ones grows wider as u_6 increases. The same type of behavior is realizable for $g<0$ and $m \to n-m$.

VII. PRELIMINARY RG ANALYSIS OF THE TRICRITICAL REGION

In the limit $g \ll 1$ the integration over $\vec{S}_{n-m}$ (if initially $r_{n-m} \gtrsim r_m$) can be performed only after l^* iterations (see Sec. III). At this point one has $r_{n-m}(l^*) \simeq O(1)$, which allows the elimination of the noncritical $(n-m)$-components [using a simple perturbation expansion in powers of $u_4(l^*)$, $v(l^*)$, $u_6(l^*)$, $x(l^*)$, and $y(l^*)$] to obtain an effective m-component cubic Hamiltonian of exactly the same form as (50) and (51) in which all the coefficients are l^* dependent. We then locate the tricritical point using the tricriticality condition (54), i.e., $W_{\text{eff}}(m,l^*) \simeq 0$. The answers, obtained in terms of the renormalized parameters $[u_4(l^*),v(l^*),u_6(l^*),x(l^*),y(l^*)]$ are then related to the initial parameters $[u_4,v,u_6,x,y]$ by solving the recursion relations of the RG transformation.

When $g \neq 0$ $(g \gtrsim 0)$, the quadratic term $(r|\vec{S}|^2)/2$ in the GLW Hamiltonian (50) splits into two terms, i.e.,

$$(r_m|\vec{S}_m|^2+r_{n-m}|\vec{S}_{n-m}|^2)/2\,,$$

with r_m and r_{n-m} defined in Sec. III. Under the iteration of the RG, (35) and its renormalized counterpart $\mathscr{H}(l)$ remain in the same parameter space to leading order in ϵ. To $O(\epsilon,u_6,x,y)$ the differential RG recursion relations for $r_m(l)$ and $r_{n-m}(l)$ are given by Eqs. (20) and (21) (with K_d replaced by K_4) to which new contributions (generated by v), i.e., $12K_4v(1-r_m)$ and $12K_4v(1-r_{n-m})$, respectively, have to be added. Provided that $r_m(l)$ and $r_{n-m}(l)$ do not become *too large* [i.e., $r_i(l) \lesssim O(1)$, $i=m,n-m$], the RG flows in the (u_4,v,u_6,x,y) space are not affected [to $O(\epsilon)$] by the breaking of the isotropic quadratic symmetry. This implies that Eqs. (38)–(42) are still applicable. The equations for $r_m(l)$ and $r_{n-m}(l)$ can be solved by the same procedure adopted in Sec. IV, namely by reintroducing the original variables $r(l)$ and $g(l)$, which decouple the recursion relations for $r_m(l)$ and $r_{n-m}(l)$. Under the RG transformation the evolution of r and g is given by[27]

$$\frac{dr}{dl}=2r+4(n+2)K_4u_4(1-r)+12K_4v(1-r)\ , \qquad (58)$$

$$\frac{dg}{dl}=2g-8K_4u_4g-12K_4vg\ . \qquad (59)$$

Given $u_4(l)$ and $v(l)$, the solutions of (58) and (59) are obtained with the use of methods similar to those in Ref. 17. Defining $\Delta u_4(l)=u_4(l)-u_4^C$ and $\Delta v(l)=v(l)-v_C$, the solutions may be written

$$g(l)=\exp(\lambda_g l)\bar{g}(l)\ ,$$
$$\bar{g}(l)=g(0)\exp\left[-\int_0^l[8K_4\Delta u_4(l')+12K_4\Delta v(l')]dl'\right]\ , \qquad (60)$$

and

$$r(l)=t(l)-2(n+2)K_4u_4(l)-6K_4v(l)\ ,$$
$$t(l)=\exp(\lambda_t l)\bar{t}(l)\ , \qquad (61)$$
$$\bar{t}(l)=t(0)\exp\left[-\int_0^l[4(n+2)K_4\Delta u_4(l')+12K_4\Delta v(l')]dl'\right]\ , \qquad (62)$$

where the eigenvalues[27]

$$\lambda_t=2-[2(n-1)/3n]\epsilon\ ,$$
$$\lambda_g=2-[(n-2)/3n]\epsilon \qquad (63)$$

correspond to the unstable borderline cubic fixed point

$$u_4^C=[1/12K_4n]\epsilon\ ,$$
$$v_C=[(n-4)/36K_4n]\epsilon\ , \qquad (64)$$
$$u_6^C=x_C=y_C=0\ .$$

To solve for $u_4(l)$ and $v(l)$ we first transform to $\tilde{u}_4(l)$ [Eq. (43)] and $\tilde{v}(l)$ [Eq. (44)]. Their respective equations (46) and (47) have been solved some years ago in Ref. 17 with the use of techniques developed by Rudnick.[14] The solutions are parametric[14,17] and cannot be expressed as simple functions of l. In principle, given $\tilde{u}_4(l)$ and $\tilde{v}(l)$ we can solve Eqs. (40)—(42) with u_4 and v replaced by $\tilde{u}_4$ and $\tilde{v}$ to obtain $u_6(l)$, $x(l)$, and $y(l)$ (generally the solutions will again be parametric). Given $\tilde{u}_4(l)$, $\tilde{v}(l)$, $u_6(l)$, $x(l)$, and $y(l)$ as functions of l, one transforms back to $u_4(l)$ and $v(l)$ and afterwards solves for $\bar{t}(l)$ and $\bar{g}(l)$ in Eqs. (60) and (61). We should like to emphasize that in the cubic problem it would be quantitatively erroneous to linearize the equations for g, t, u_4, v, u_6, x, and y in the vicinity of the unstable cubic fixed point to calculate universal amplitude ratios. This follows from the fact that the RG flow takes the system away from the linear region, and it is precisely in that region where tricriticality occurs. Note that in the isotropic case (Sec. III) the assumption $\tilde{u}_4(0)/\tilde{u}_4^H\ll 1$ was in a sense equivalent to a linearization in the vicinity of the Gaussian fixed point; however, in that case the assumption was justified (as was checked explicitly) because tricriticality occurred in a region close to the n-component tricritical line $\tilde{u}_4(0)=0$, and still far from the stable Heisenberg fixed point. Although in the cubic problem the situation is different (because the RG flow takes the system away from any stable fixed point), an analysis based on a linearization in the vicinity of the cubic fixed point will still produce all the relevant *qualitative* features and serve as a preliminary starting point for a more complete analysis of the problem. In particular, the various exponents obtained from such an analysis should be correct because these should depend only on the nature of the fixed point.

Linearizing Eqs. (58), (59), (46), and (47) about the cubic fixed point, we obtain

$$g(l)=ge^{\lambda_g l}\ , \qquad (65)$$

$$t(l)=t(0)e^{\lambda_t l},\quad t(0)=r+2(n+2)K_4u_4+6K_4v\ , \qquad (66)$$

$$\tilde{u}_4(l)=u_4^C+[2(4-n)/(n+2)]\times[3W_1(l)/(4-n)-W_2(l)/2]\ , \qquad (67)$$

$$\tilde{v}(l)=v_C-[2(4-n)/(n+2)][W_1(l)-W_2(l)]\ , \qquad (68)$$

where

$$W_1(l)=W_1(0)e^{\lambda_1 l}\ ,$$
$$W_1(0)=\tilde{u}_4+\tilde{v}/2-[(n-1)/36K_4n]\epsilon\ , \qquad (69)$$
$$\lambda_1=-\epsilon$$

$$W_2(l)=W_2(0)e^{\lambda_2 l}\ ,$$
$$W_2(0)=W(n)=\tilde{u}_4+3\tilde{v}/(4-n)\ , \qquad (70)$$
$$\lambda_2=[(4-n)/3n]\epsilon$$

and λ_g, λ_t, u_4^C, and v_C were defined, respectively, in Eqs. (63) and (64).

Linearization of Eqs. (40)—(42) now yields

$$\begin{bmatrix}u_6'\\x'\\y'\end{bmatrix}=(-2+2\epsilon)\begin{bmatrix}u_6\\x\\y\end{bmatrix}-\frac{\epsilon}{3n}\begin{bmatrix}6(n+5) & 0 & 6\\12(n-4) & 15(n-1) & (n-7)\\12(n-4) & 15 & (8n-5)\end{bmatrix}\begin{bmatrix}u_6\\x\\y\end{bmatrix}\ . \qquad (71)$$

The three eigenvalues associated with these equations may be written as

$$\lambda_{6,i} = -2+2\epsilon-\epsilon x_i/3n + O(\epsilon^2) , \quad (72)$$

where x_i are the roots of the cubic equation

$$x^3-(29n+10)x^2+(258n^2+288n-132)x -(720n^3+1260n^2+1260n-3240)=0 . \quad (73)$$

For $n=1$ this has a single real root, $x=0$, recovering the expected Gaussian eigenvalue $\lambda_6 = -2 + 2\epsilon$.[24] For $n=2$ the roots are $x_i = 14$, 24, and 30, i.e., $\lambda_{6,i} \simeq -2-\epsilon/3, -2-2\epsilon, -2-3\epsilon$. For $n=3$ we find $x_i = (67\pm\sqrt{313})/2$, and 30, i.e., $\lambda_{6,i} \simeq -2-0.7393\epsilon$, $-2-2.7051\epsilon, -2-4\epsilon/3$. Similar solutions can be worked out for higher values of n, but the cubic and Heisenberg fixed points are expected to interchange roles for $n \geq 4$.[3,24]

The initial values of u_6, x, and y may now be expanded in terms of the eigenvectors of the above eigenvalues. After a large number of iterations, $(u_6(l), x(l), y(l))$ will be approximately proportional to the eigenvector of the least negative eigenvalue, i.e., $\lambda_{6,i} \simeq -2-a(n)\epsilon$, with $a(2) = \frac{1}{3}$ and $a(3) \simeq 0.7393$. Having calculated the corresponding eigenvectors, we find

$$(u_6(l), x(l), y(l)) \rightarrow \tilde{w}(1, b_x(n), b_y(n)) e^{\lambda_{6,1} l} , \quad (74)$$

with

$$b_x(2) = \tfrac{2}{3}, \quad b_y(2) = -\tfrac{14}{3} ,$$
$$b_x(3) = -\tfrac{2}{3}, \quad b_y(3) \simeq -3.891 .$$

The coefficient $\tilde{w}$ is equal to a linear combination of $u_6(0)$, $x(0)$, and $y(0)$ which represents the projection on this eigenvector,

$$\tilde{w} = 0.45u_6 + 0.5625x - 0.0375y, \quad n=2$$
$$\tilde{w} = 0.3148u_6 + 0.9516x - 0.3391y, \quad n=3 . \quad (75)$$

In what follows we shall assume that $\tilde{w} < 0$.

Having solved the recursion relations in the linear regime we select a value of l^* by requiring[17] (24) with $t(l)$ and $g(l)$ given, respectively, in (66) and (65). At that point the renormalized Hamiltonian $\mathcal{H}(l^*)$ is noncritical with respect to fluctuations in $\vec{S}_{n-m}$ which are then eliminated in the usual way (Sec. III) to obtain the effective m-component cubic Hamiltonian (50). The various parameters in (50) (which now depend on l^*) are given by Eqs. (14)–(16), (52), and (53). In $\mathcal{H}_{\rm eff}(l^*)$ we easily identify a temperaturelike variable $t_{\rm eff} = r_{\rm eff} = O(\epsilon)$. Tricriticality ($t$) will be obtained when $t_{{\rm eff},t} = W_{{\rm eff},t}(m) \simeq 0$. To leading order, the condition $t_{{\rm eff},t} \simeq 0$ implies Eq. (25) with $t(l)$ and $g(l)$ given, respectively, in (66) and (65). Finally, the condition (54), i.e., $W_{{\rm eff},t}(m) \simeq 0$, is imposed with $\tilde{u}_4(l)$, $\tilde{v}(l)$, $u_6(l)$, and $y(l)$ given, respectively, in (67), (68), and (74). One should note, however, that the term of $O(u_4^2) \simeq O(\epsilon^2)$ in (54) is of higher accuracy than the one we have been working with, i.e., $O(\epsilon)$, throughout this calculation, and therefore should be neglected. Recall that in the large-g limit analysis of this term was responsible for the existence of an additional tricritical point (see Sec. VI); however, in the $g \ll 1$ limit the mechanism is different. Substituting (25) from (26) we obtain $g(l^*) \simeq 1$, which [with the use of (65)] implies

$$e^{l^*} \simeq g^{-1/\lambda_g} . \quad (76)$$

Equation (54) now becomes

$$u_4(l^*) + 3v(l^*)/(4-m) + C(m)u_6(l^*) + B(m)x(l^*) + A(m)y(l^*) + 3(n-m)I_1(1)[u_6(l^*) + y(l^*)/(4-m)] \simeq 0 . \quad (77)$$

Substituting $\tilde{u}_4$ and $\tilde{v}$ from (43) and (44), this becomes

$$\tilde{u}_4(l^*) + 3\tilde{v}(l^*)/(4-m) - \tfrac{3}{2}K_4(n-m)\ln 2\, u_6(l^*) - \tfrac{3}{2}\ln 2 K_4(n-m) y(l^*)/(4-m) . \quad (78)$$

We now argue that for large l^* one may replace $u_6(l^*)$, $x(l^*)$, and $y(l^*)$ by their limiting behavior [Eq. (74)]. Inserting also the values for $\tilde{u}_4(l)$, $\tilde{v}(l)$, and $\exp(l^*)$ the tricriticality (t) condition (78) becomes

$$A g_t^{\psi_1} + B g_t^{\psi_2} - C g_t^{\psi_3} + W_{2t}(0) \simeq 0 , \quad (79)$$

where

$$\psi_1 = \lambda_2/\lambda_g = [(4-n)/6n]\epsilon, \quad \psi_2 = (\lambda_2-\lambda_1)/\lambda_g = [(4+2n)/6n]\epsilon ,$$
$$\psi_3 = (\lambda_2-\lambda_{6,1})/\lambda_g = 1 + [(1/3n) + a(n)/2]\epsilon , \quad (80)$$

i.e., $\psi_3 = 1 + \epsilon/3$ for $n=2$ and $\psi_3 = 1 + 0.4808\epsilon$ for $n=3$. The coefficients in (79) are given by

$$A=\{[3(n-m)(n+2)]/[(4-n)^2(m+2)]\}(-v_C),\quad B=\{[6(n-m)]/[(4-n)(m+2)]\}W_1(0)\,,$$
$$C=[(n-m)(4-m)(n+2)K_4]/[2(4-n)(m+2)][3\ln 2+3\ln 2b_y(n)/(4-m)]\widetilde{w}\,. \tag{81}$$

Note that in the regions of interest A, B, and C are positive whereas $W_2(0)<0$. When $g \to 0^+$, the first term dominates the g dependence ($\psi_1<\psi_2<\psi_3$) of Eq. (79), and we obtain

$$W_{2t}(0)=W_t(n)=[\widetilde{u}_4+3\widetilde{v}/(4-n)]_t \propto g_t^{\psi_1}\,, \tag{82}$$

where we have deliberately not written the amplitude explicitly to emphasize that the present calculation is only correct *qualitatively* for nonuniversal features. Note that the relation $\psi_1=\lambda_2/\lambda_g$, which depends only on the nature of the cubic fixed point, is *quantitatively* correct (in fact it could be obtained from scaling arguments in the vicinity of the unstable cubic fixed point). Moreover, since $\psi_1<1$, it follows that the line of tricritical points approaches the ($g=0$) tricritical point $W(n)=0$ (points A and B in Fig. 6) tangentially to the u_4 axis. Eqs. (82) and (48) show that as u_6 (>0) is increased for given values of u_4, v, x, and y, the tricritical points occur for lower values of g_t (see Fig. 6). Similarly, for given g, v, x, and y, u_{4t} is shifted towards lower values (e.g., from A to B in Fig. 6) as u_6 (>0) is increased.

From Eq. (79) it is clear that there is a range of values for $W_2(0)=W(n)$ for which *two* solutions (g_{t1} and g_{t2}) exist. Note that the new effect predicted here is expected to occur in regions below the m-component tricritical plane, i.e., for $|W_2(0)|>|W(m)|$. This follows from the fact that the function

$$F(g_t)=Ag_t^{\psi_1}+Bg_t^{\psi_2}-Cg_t^{\psi_3}$$

grows initially (due to the first two terms) reaching to its maximum at g_t^* and then bends back (due to the last negative term). It follows then that for $|W(m)|\le|W_{2t}(0)|<F(g_t^*)$, the line $-W_{2t}(0)=\text{const}$ will intersect the curve $F(g_t)$ *twice,* thus yielding two tricritical points.

In this section we have presented a preliminary RG analysis through which we tried to show the qualitative mechanism leading to two consecutive tricritical points. In terms of RG flows, one should note that although u_6, x, and y are irrelevant (decaying to zero for sufficiently large l), they may drive $[\widetilde{u}_4+3\widetilde{v}/(4-m)]$ towards higher values in the first few iterations. Later, v takes over (being relevant near the unstable cubic fixed point) in driving u_4 towards negative values. If one starts sufficiently close to the m- [or $(n-m)$-] component tricritical plane and below it (just outside region a of Fig. 4), then the RG flow crosses the plane twice. In region b of Fig. 4 the RG flow will drive the system towards the m-component tricritical plane, and therefore we again predict the diagrams of Figs. 2(b) and 2(c).

It is worthwhile emphasizing that all our results were based on the model Hamiltonian (35) in which many higher-order terms were ignored. Although these higher-order terms are irrelevant, they are expected to modify the scaling fields and thus change explicit expressions like (48). However, they will not change the qualitative features of the phase diagrams. Because of these additional irrelevant terms, one should not apply our conditions for obtaining these diagrams, e.g., $u_6+y/(4-m)>0$ or $\widetilde{w}<0$, directly to real systems. Particular cubic systems (with $v<0$) may exhibit any one of the diagrams in Figs. 2 and 5.

It should also be emphasized that we have ignored here explicit direct dependence of u_4, v, u_6, x, and y on the anisotropy g. Such dependences may yield the diagrams of Figs. 2 and 5 already within Landau's theory. However, Fig. 5 will be obtained within Landau's theory only if (u_4+v) has a very special dependence on g (it must change its sign twice). Such restrictions are not necessary in our theory. In addition, fluctuations will modify the shapes of the diagrams and the related amplitude ratios.

VIII. EXPERIMENTAL REALIZATIONS

To observe the new crossover predicted in Figs. 2(b) and 2(c) we must search for isotropic n-component systems which are also tricritical and may be subjected to symmetry-breaking mechanisms of the type given in (12) (for a discussion see Sec. III). All ($n=2$)- and ($n=3$)-component physical systems that we are aware of fail to enter this category. The system of ^3He-^4He mixtures[28(a)–28(c)] is described by an ($n=2$)-component isotropic model[28(d)] which exhibits a tricritical point. However, there is no experimentally available quadratic symmetry-breaking mechanism to break the symmetry of the *complex* order parameter associated with the superfluid transition. Transitions to incommensurate phases,[29] e.g., in K_2SeO_4 (see Ref. 30) where the phason mode is unpinned, are usually described by isotropic ($n=2$)-component models. In such cases, however, the relevant quantity is again the phase of a complex order parameter and we run into the same problems as before, even if the system could be made tricritical (which is difficult in itself). In fact, most tricritical systems in nature are of the *Ising* ($n=1$) type, e.g., compounds undergoing *structural* phase transitions such as ND_4Cl,[31] NH_4Cl,[32] the α-β transition in quartz,[33] metamagnetic systems such as $FeCl_2$,[34] etc. Obviously in this case the symmetry cannot be broken.

It is therefore necessary to consider ($n \geq 4$)-component systems.[10,11] These systems are characterized by *complex symmetries* and exhibit fluctuation-driven first-order transitions due to the lack of an accessible and/or stable fixed point. Their critical behavior is not characteristic of an isotropic system (the GLW Hamiltonians which describe these compounds contain a number of fourth-order invariants[10,11]). However, under suitable symmetry breaking they will behave effectively as an isotropic system which can be made tricritical. A subsequent breaking of the symmetry will produce the new crossover predicted in this paper. A possible realization of this type is the fcc type-II antiferromagnetic compound MnO ($n=8$).[11,18] A uniaxial stress $p > p_t \simeq 5$ kbar (Ref. 21) along the [111] direction turns the fluctuation-driven first-order transition of the eight-component antiferromagnetic order parameter into a continuous one described by an *hexagonal* two-component (S_1, S_2) order-parameter vector [in the (111) plane].[18] Note that in a hexagonal system the isotropy is broken only in the sixth- and higher-order terms [for example, in the present case (two-component system)]; there is an additional term $(S_1^3 - 3S_1S_2^2)^2$ which is invariant under rotations of 60°. We believe that this should not alter our predictions. Moreover, other compounds with hexagonal symmetry, which show tricriticality and can be subjected to quadratic symmetry breaking may provide additional experimental test grounds for our predictions. For $p \gtrsim p_t$ we predict that a magnetic field (which in an antiferromagnet couples quadratically to the order parameter) in the (111) plane will yield Figs. 2(b), 2(c), and 3 (u_4 is represented here by p, $n=2$, and $m=1$).

To realize two consecutive tricritical points [Figs. 5(b) and 5(c)] we must look for cubic compounds undergoing first-order cubic-to-tetragonal phase transitions ($v<0$) which can be made *tricritical* and in which the symmetry can be broken as in (12). We suggest that the perovskite-type compounds $BaTiO_3$ (Ref. 26) or $KTa_xNb_{1-x}O_3$ (KTN) (Ref. 35) may be suitable candidates. Increasing the hydrostatic pressure on $BaTiO_3$ (Ref. 36) or the concentration x in KTN (Ref. 35) moves the parameters u_4, v, u_6, x, and y through the n-component tricritical surface $W(n)=0$ given in (48), crossing in their way the m-component tricritical surface $W(m)=0$ (for $g>0$) or the $(n-m)$-component one (for $g<0$). Note that this is achieved without breaking the symmetry of the order parameter, but rather via a renormalization of the various parameters through their dependence on p or x. As this pressure (concentration) is increased we predict that additional uniaxial stress along, e.g., [100], will yield the sequence of diagrams shown in Figs. 5(a)—5(c) and 2(a) ($n=3, m=1,2$).

In a recent experiment[37] a phase diagram like the one shown in the upper part of Fig. 5(c), with $m=1$, has been found for the compound $KMnF_3$ under uniaxial stress along [100]. This perovskite crystal[38] (with $v<0$) is also a suitable candidate. In fact, in some sense it is even better than $BaTiO_3$ because it undergoes a weak first-order transition ($BaTiO_3$ exhibits a strong one). This implies that the parameters in $KMnF_3$ are probably close to the regions in which the new effects are predicted to occur, whereas in $BaTiO_3$ they are not (a hydrostatic pressure of about 33 kbar is required to obtain a tricritical point[36]). In the above-mentioned experiment no hydrostatic pressure was needed, which confirms our arguments. We may say that the parameters in $KMnF_3$ lie in the region just below the Ising ($m=1$)-component tricritical surface (which is also the instability surface). However, we must emphasize that in $KMnF_3$ there is an additional complication (not taken into account in the present analysis)—its Lifshitz[39,22] character, which could affect the phase diagrams. We believe (and the experiment confirms this in some sense) that at least qualitatively our conclusions should remain unchanged for $m=1$ (for $m>1$ there is no accessible fixed point for Lifshitz systems of cubic symmetry and the transition is expected to remain first order[22]).

Another possible realization of Figs. 5(b) and 5(c) is TbP.[11,20,40] A uniaxial stress or a magnetic field along [111] may turn this $n=4$ fluctuation-driven first-order transition into an $n=3$ (cubic) continuous one. Additional uniaxial stress along $[\bar{1}11]$, $[\bar{1}\bar{1}1]$, or $[1\bar{1}1]$ will then yield our new effect.

IX. CONCLUDING REMARKS

In the present paper we have shown that critical fluctuations are able to driven an otherwise *first-order* transition (predicted by Landau theory which neglects fluctuations) into a *continuous* one. We have denoted this new type of phase transition as fluctuations-driven continuous. We have shown that they will always occur near tricritical points of isotropic n-component spin systems.

Subsequently, we have shown that by applying a mechanism which tends to weaken the critical fluctuations such as a quadratic symmetry-breaking field g, the fluctuation-driven continuous transition becomes first order beyond a tricritical point, as in Figs. 2(b) and 2(c). We would like to emphasize that additional mechanism, which do not necessarily break the symmetry of the order parameter, but nevertheless weaken critical fluctuations, are possible. For example, we have recently shown[41] that application of hydrostatic pressure or uniaxial stress perpendicular to the layered structure of some metamagnetic[42] compounds (these do not break the symmetry of the order parameter) such as $FeCl_2$, may induce new types of tricritical points (at which the order of the phase transition changes). This new type of crossover follows from the weakening of critical fluctuations due to a dimensionality shift from $d \simeq 2$ to 3 (see also Ref. 43). Additional mechanisms, such as increasing the range of the interactions, inducing a change from quantum to classical behavior, weakening of random linear fields, etc., which tend to weaken fluctuations, may induce similar effects.

Moreover, we have shown that in systems which show fluctuation-driven first-order transitions (which occur near tricritical points), there is a range in which the symmetry breaking first turns the fluctuation-driven first-order transition into a continuous one, and then turns it back into first order, via two consecutive tricritical points [Figs. 5(b) and 5(c)].

A very important conclusion from the present analysis is that under certain conditions (e.g., negative fourth-order terms), higher-order (e.g., sixth-order) terms in the GLW Hamiltonian (which are usually neglected due to their irrelevance in the RG sense) may play a crucial role. We have stressed that although such variables (usually called "dangerous" irrelevant variables) are incapable of affecting the asymptotic critical behavior, they may prevent it from occurring at all.

In this paper we limited the discussion to $v<0$ and $u_4+v>0$, so that the ordered phases near the transitions are tetragonal. As we mentioned in Sec. V, the sixth-order terms may cause additional transitions at lower temperatures, e.g., into the orthorhombic phase. A full analysis within the ordered phases is left for future studies.

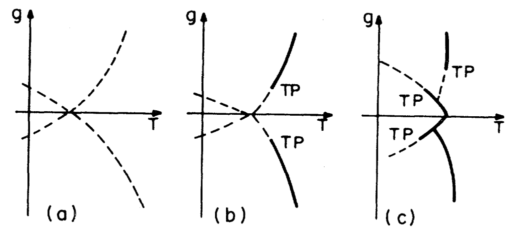

FIG. 7. Conjectures schematic (g,T) tetracritical phase diagrams for the cubic problem with $v>0$. Notation is as in Fig. 2.

The assumption that $v<0$ ensured that the phase diagrams exhibited a *bicritical point* [Fig. 2(a)]. When $v>0$ (and $u_4>0$), *tetracritical points* are expected [Fig. 7(a)].[25] When the tetracritical point occurs near the n-component tricritical point (on its continuous side), calculations similar to those of Secs. III and IV will modify Fig. 7(a) into Fig. 7(b). When the n-component system has a first-order transition then the situation becomes more complicated[20] and the phase diagram probably turns into Fig. 7(c). Detailed calculations within the ordered phases here are also left for the future.

In conclusion, we have shown that the interplay between critical fluctuations, dangerous irrelevant variables, and symmetry-breaking mechanisms yields many new kinds of tricritical points. We hope that the large number of physical realizations that were suggested in Sec. VIII will stimulate further experimental checks on our predictions.

ACKNOWLEDGMENTS

We have enjoyed discussions with D. Mukamel and K. A. Müller. This work was supported by the U.S.—Israel Binational Science Foundation. D. B. acknowledges the award of a Sir Charles Clore Fellowship.

---

*Present address: Department of Physics, Massachusetts Institute of Technology, Cambridge, MA 02139.

[1]L. D. Landau and E. M. Lifshitz, *Statistical Physics,* 2nd ed. (Peragmon, New York, 1968), Chap. XIV.

[2]K. G. Wilson and J. Kogut, Phys. Rep 12C, 75 (1974).

[3]See, e.g., A. Aharony, in *Phase Transitions and Critical Phenomena,* edited by C. Domb and M. S. Green (Academic, New York, 1976), Vol. 6, p. 357, and references therein.

[4]R. B. Griffiths, Phys. Rev. Lett. 24, 715 (1970).

[5]F. J. Wegner and A. Houghton, Phys. Rev. A 8, 401 (1973).

[6]D. R. Nelson and J. Rudnick, Phys. Rev. Lett. 35, 178 (1975); J. Rudnick and D. R. Nelson, Phys. Rev. B 13, 2208 (1976).

[7]E. K. Riedel and F. J. Wegner, Phys. Rev. Lett. 29, 349 (1972); F. J. Wegner and E. K. Riedel, Phys. Rev. B 7, 248 (1973).

[8]M. J. Stephen and J. McCauley, Phys. Lett. 44A, 193 (1973).

[9]D. Blankschtein and A. Aharony, Phys. Rev. Lett. 47, 439 (1981).

[10]P. Bak, S. Krinsky, and D. Mukamel, Phys. Rev. Lett. 36, 52 (1976).
[11]D. Mukamel and S. Krinsky, Phys. Rev. B 13, 5056, 5078 (1976); P. Bak and D. Mukamel, Phys. Rev. B 13, 5086 (1976).
[12]S. A. Brazovskii and I. E. Dzyaloshinskii, Pis'ma Zh. Teor. Fiz. 21, 360 (1975) [JETP Lett. 21, 164 (1975)].
[13]T. Nattermann and S. Trimper, J. Phys. A 8, 2000 (1975).
[14]J. Rudnick, Phys. Rev. B 18, 1406 (1978).
[15]M. E. Fisher, in *Magnetism and Magnetic Materials—1974 (San Francisco),* Proceedings of the 20th Annual Conference on Magnetism and Magnetic Materials, edited by C. D. Graham, Jr., and G. H. Lander (AIP, New York, 1975), p. 273.
[16]A. Aharony and A. D. Bruce, Phys. Rev. Lett. 33, 427 (1974).
[17]E. Domany, D. Mukamel, and M. E. Fisher, Phys. Rev. B 15, 5432 (1977).
[18]P. Bak, S. Krinsky, and D. Mukamel, Phys. Rev. Lett. 36, 829 (1976).
[19]S. J. Knak Jensen, O. G. Mouritsen, E. K. Hansen, and P. Bak, Phys. Rev. B 19, 5886 (1979).
[20]M. Kerszberg and D. Mukamel, Phys. Rev. Lett. 43, 293 (1979); Phys. Rev. B 23, 3943, 3953 (1981).
[21]D. Bloch, D. Hermann-Ronzaud, C. Vettier, W. B. Yelon, and R. Alben, Phys. Rev. Lett. 35, 963 (1975).
[22]J. Y. Buzaré, J. C. Fayet, W. Berlinger, and K. A. Müller, Phys. Rev. Lett. 42, 465 (1979); A. Aharony and A. D. Bruce, Phys. Rev. Lett. 42, 462 (1979).
[23]D. R. Nelson and E. Domany, Phys. Rev. B 13, 236 (1976).
[24]A. Aharony, Phys. Rev. B 8, 4270 (1973).
[25]A. D. Bruce and A. Aharony, Phys. Rev. B 11, 478 (1975).
[26]A. F. Devonshire, Adv. Phys. 3, 85 (1954).
[27]A. Aharony, Phys. Lett. 59A, 163 (1976).
[28](a) E. H. Graf, D. M. Lee, and J. D. Reppy, Phys. Rev. Lett. 19, 417 (1967); (b) T. A. Alvesalo, P. Berglund, S. Islander, G. R. Pickett, and W. Zimmermann, Jr., Phys. Rev. A 4, 2354 (1971); (c) G. Goellner, R. Behringer and H. Meyer, J. Low-Temp. Phys. 13, 113 (1973); (d) A. N. Berker and D. R. Nelson, Phys. Rev. B 19, 2488 (1979).
[29]For a review, see, e.g., A. D. Bruce, Adv. Phys. 29, 111 (1980), and references therein.
[30]M. Iizumi, J. D. Axe, G. Shirane, and K. Shimaoda, Phys. Rev. B 15, 4392 (1977).
[31]W. B. Yelon, D. E. Cox, and A. Linz, Phys. Rev. 177, 848 (1969); W. C. Garland and J. D. Baloga, Phys. Rev. B 16, 331 (1977).
[32]C. W. Garland and B. B. Weiner, Phys. Rev. B 3, 1634 (1971); W. B. Yelon, D. E. Cox, P. J. Kortman, and W. B. Daniels, Phys. Rev. B 9, 4843 (1974).
[33]E. J. K. B. Banda, R. A. Craven, R. D. Parks, P. M. Horn, and M. Blume, Solid State Commun. 17, 11 (1975).
[34]R. J. Birgeneau, G. Shirane, M. Blume, and W. C. Koehler, Phys. Rev. Lett. 33, 1098 (1974); J. A. Griffin and S. E. Schnatterly, Phys. Rev. Lett. 33, 1576 (1974).
[35]L. T. Todd, Jr., M. Sc. thesis, Massachusetts Institute of Technology, 1970 (unpublished); S. K. Kurtz, Bell Syst. Tech. J. 65, 1209 (1966).
[36]G. Samara, Ferroelectrics 2, 277 (1971); R. Clarke and L. Benguigui, J. Phys. C 10, 1963 (1977).
[37]S. Stokka, K. Fossheim, and V. Samulionis, Phys. Rev. Lett. 47, 1740 (1981); S. Stokka and K. Fossheim, J. Phys. C 15, 1161 (1981).
[38]G. Shirane, V. J. Minkiewicz, and A. Linz, Solid State Commun. 8, 1941 (1970).
[39]R. M. Hornreich, M. Luban, and S. Shtrikman, Phys. Rev. Lett. 35, 1678 (1975).
[40]E. Bucher, J. P. Maita, G. W. Hull, Jr., L. D. Longinotti, E. Lüthi, and P. S. Wang, Z. Phys. B 25, 41 (1976); F. Levy, Phys. Kondens. Mater. 10, 85 (1969).
[41]D. Blankschtein and A. Aharony, Phys. Rev. B 26, 415 (1982).
[42]For a general review on metamagnetic compounds, see, e.g., E. Stryjewski and N. Giordano, Adv. Phys. 26, 487 (1977).
[43]Y. Shnidman and E. Domany, J. Phys. C 14, L773 (1981).